

# Bending Stress and Deflection Analysis of Meshing Spur Gear Tooth during the Single Tooth Contact with Finite Element Method and Determination of the Bending Stiffness

Antonios D. Tsolakis, Konstantinos G. Raptis and Maria D. Margaritou

Department of Mechanical Engineering, School of Applied Sciences and Technology,  
Piraeus University of Applied Sciences, 250 Thivon and P. Ralli, 12244, Egaleo, Greece

## Article history

Received: 03-11-2015

Revised: 18-05-2017

Accepted: 02-06-2017

## Corresponding Author:

Antonios D. Tsolakis  
Department of Mechanical  
Engineering, School of Applied  
Sciences and Technology,  
Piraeus University of Applied  
Sciences, 250 Thivon and P.  
Ralli, 12244, Egaleo, Greece  
Email: adtsolakis@gmail.com

**Abstract:** Purpose of this study is the study of loading and contact problems encountered at rotating machine elements and especially at tooth gears. Tooth gears are some of the most commonly used mechanical components for rotary motion and power transmission. This fact proves the necessity for improved reliability and enhanced service life, which requires precise and clear knowledge of the stress field at gear tooth. This study investigates three different study cases of the stresses occurring during the single tooth meshing, regarding the gear module, power rating and number of teeth as variable parameters. Using finite elements analysis, the stresses and deflections on discrete points of contact are derived. Finally from the finite elements analysis results calculated the peripheral bending stiffness of the loaded tooth. From FEM analysis and analytical calculation the magnitudes of root stresses, contact displacement and peripheral bending stiffness, during the single tooth contact, are presented with graphs versus the height of the contact to the total tooth height ratio. During the single tooth contact the values of the Equivalent and 1st principal stress at the addendum of the tooth, the bending deflection and the peripheral bending stiffness at the point of contact are proportional to the height of the contact in respect of the total tooth height.

**Keywords:** Gears, Gears Tooth, Highest Point of Single Tooth Contact (HPSTC), Bending Stresses, Bending Deflection, Finite Element Method (FEM)

## Introduction

Most mechanical systems including gear sets are sensitive to operating conditions such as excessive applied torque, bad lubrication and manufacturing or installation problems. When the tooth surfaces are subjected to excessive stress conditions, failure of the tooth surface may occur. This can cause removal and plastic deformation of the contacting tooth surfaces and fatigue crack apparition. Many works have been carried out to calculate this stiffness. Finite Elements Models (FEM) are the most popular tools used to do this. However, analytical methods showed good results in calculating tooth stiffness. They offer satisfying results, good agreements compared with FEM and reduced computation time (Fakher *et al.*, 2009).

First systematic attempt to calculate the position of critically stressed point is attributed to Lewis (1882), who considered that the inscribed isosceles parabola tangent to the dedendum of the tooth flank defines the critically stressed point which is located at the point of tangency at the side which is loaded by tensile stresses.

Methods, such as AGMA standard and DIN (Kawalec *et al.*, 2006), Heywood's semi-empirical method (Heywood, 1962) and Dolan and Broghamer's (1942) empirical formula, can be found on references and are recommended for the determination of the precise stress level caused by the phenomenon of the stress concentration at gear tooth root.

According to method proposed by DIN 3990 (1987) and ISO 6336:3 (1996), standards, the bending stresses calculation at gear tooth root is based on the concept of

“30°C tangent”, (Heywood, 1962), which proves to be a disadvantage. Thus, this method is quite approximate and should not be applied to the design of high load gearings.

Heywood’s method (Heywood, 1962), is applied for the determination of maximum real stress at critically stressed point at the root of a stubby beam with constant width. This method was later modified in order to make more precise prediction of the critical point which is located at a lower position from then on.

## Materials and Methods

The previously mentioned methods of maximum stress calculation at gear tooth root will not be applied to the present study, because the determination of the necessary geometric features, especially at the critical region of gear tooth fillet which requires more precise computations, is a time-consuming procedure. Instead, the applied method assumes that the maximum load during gear tooth meshing is applied to the Highest Point of Single Tooth Contact (HPSTC), (Spitas *et al.*, 2005; Raptis *et al.*, 2010).

### Gear Tooth Bending Stress Calculation According to the Gearing Theory

The gear tooth bending stress calculations are made separately for pinion and meshing gear tooth.

Assuming the gear tooth is a stubby cantilever beam, we calculate the stresses at gear tooth root, which are growing by the load  $F_n$  application. If we resolve load  $F_n$  into its components, there are the tangential component and the radial component. The first one, assuming that it’s a transversal load, bends the gear tooth causing bending and shear stresses while the second one, causes compressive stress. That means that there are three kind of stresses which are applying at gear tooth root. These three kinds of stresses are, the bending stress, the compressing stress and the shear stress, as seen at Fig. 1.

Since the overlap coefficient (or contact ratio) is greater than 1 ( $\epsilon > 1$ ), it means that for a certain period of the implementation, a second pair of teeth comes into engagement before the first pair breaks contact. Therefore, load  $F_n$  is acting on both pairs of teeth. As seen at Fig. 2:

- A is the point of contact at pinion root. From this point contact begins, so load  $F_n$  is distributed at two pairs of gear teeth
- B is the internal single point of contact, according to pinion. The second pair of gear tooth breaks contact on point E. That means that only a single tooth pair is in contact subjected to the total load  $F_n$  at point B

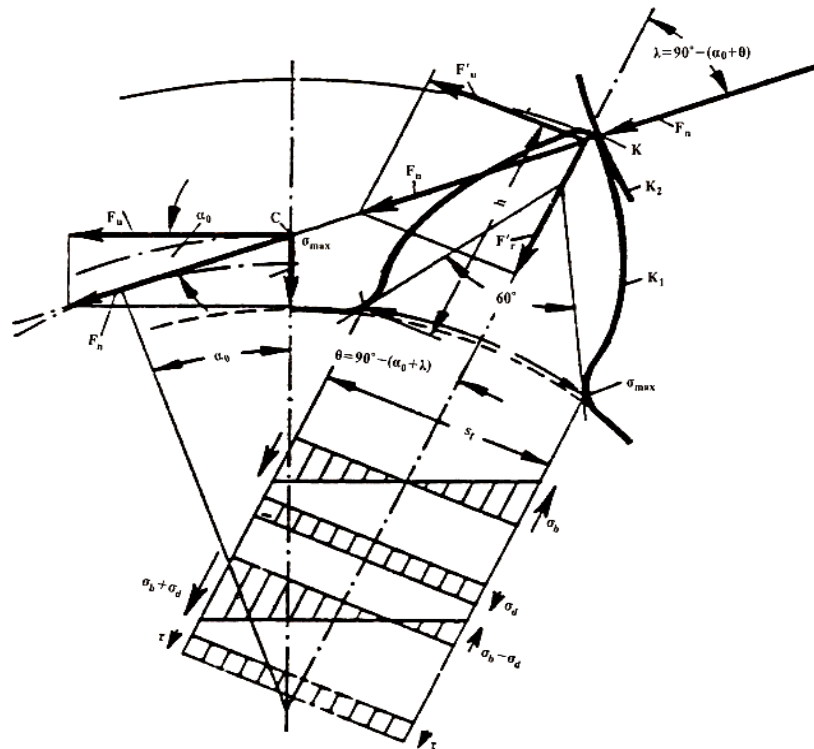


Fig. 1. Gear tooth flank loading



### Loads Applied at Pair of Gear Teeth

Assuming that only one pair of spur gear teeth is in contact during a gear tooth meshing, then gear tooth 1 profile which transmits motion, stresses gear tooth 2 profile which takes motion. Transversal load  $F_n$  which applies at the gear teeth point of contact, coincides (if we put that point on the involute of the tooth curve) with the tooth contact path n-n, which crosses the pitch point C (Fig. 3). We assume that load  $F_n$  applies at the middle of the gear tooth length  $b$ .

Load  $F_{n1}$  applies at tooth profile following a fatigue failure line direction. Ignoring the fact of friction, load  $F_{n2}$ , which is numerical equivalent with load  $F_{n1}$  but in opposite sense, set on motion gear tooth 2, following also a fatigue failure direction.

Loads  $F_{n1}$  and  $F_{n2}$ , resolve giving radial components  $F_{r1}$ ,  $F_{r2}$  and tangential components  $F_{t1}$ ,  $F_{t2}$  which transmit torque from gear tooth 1 to gear tooth 2.

The torque  $M_t$  at gear 1 with a pitch diameter  $d_1$ , is:

$$M_t = \frac{F_{t1} \cdot d_1}{2000} (N \cdot m) \quad (1)$$

The tangential load is calculated by using the equation:

$$F_{t1} = \frac{2000 \cdot M_t}{d_1} (N) \quad (2)$$

The transversal load is calculated by using the equation:

$$F_{n1} = \frac{F_{t1}}{\cos \alpha} (N) \quad (3)$$

The radial load is calculated by using the equation:

$$F_{r1} = F_{n1} \cdot \tan \alpha (N) \quad (4)$$

where,  $\alpha$  is pressure angle, is the angle between the path contact and the common tangent of the two pitch circles at pitch point C.

### Formulas for Calculating the Gear Tooth Strength

The section  $S_f$  to the dedendum of the tooth flank (Fig. 1), which affects the calculating formulas of gear tooth strength, can be calculated by using the concept of "30°C tangent" (Heywood, 1962), or the general theory. The bending stress calculation at gear tooth root is made by using the following formula:

$$\sigma_F = \frac{F_t}{b \cdot m} \cdot Y_F \cdot Y_\epsilon \cdot K_{F\alpha} \leq \sigma_{F\epsilon\pi} \quad (5)$$

The transversal load  $F_u$  is calculated by using the following formula:

$$F_u = \frac{2 \cdot M_t}{d_o} \quad (6)$$

The torque  $M_t$  is calculated by using the following formula:

$$M_t = \frac{P}{2 \cdot \pi \cdot n} \quad (7)$$

The gear tooth width is calculated by using the following formula:

$$b = m \cdot \lambda \quad (8)$$

Where:

- $\lambda$  = A direction factor which depends on the gear tooth material quality and the bear way
- $Y_F$  = A profile factor which depends on the shift and the number of gear teeth
- $Y_\epsilon$  = An overlap coefficient
- $K_{F\alpha}$  = A factor of distribution load which depends on the gear tooth material quality

### Highest Point of Single Tooth Contact (HPSTC) During Tooth Meshing

It is proven that the normal load  $P_N$  on a gear tooth is not maximum when applied at the addendum circle. As shown in Fig. 4 during gear tooth meshing, from point A where tooth contact begins to point A' of tooth contact path and from point B' to point B, where tooth contact completes, two pairs of teeth are in contact simultaneously. On the other hand, between points A' and B' only a single tooth pair is in contact subjected to the total load.

It can, thus, be assumed that the worst loading condition for a tooth of gear 1 does not occur when the load is applied to the highest addendum point (point B), because the total load is distributed to two pairs of gear teeth at this point, but when applied to point B' of contact path where only a single pair or gear teeth is meshing, (Niemann, 1982; Spitas *et al.*, 2005; Tsolakis and Raptis, 2011).

Point A' is defined The Lowest Point of Single Tooth Contact (LPSTC) and point B' is the Highest Point of Single Tooth Contact (HPSTC) for gear 1. That is, during portion A'B' of the contact path only a single tooth of each gear is loaded, whereas during portions AA' and BB' the load is distributed to the teeth of each gear. Thus, we can infer that the maximum gear tooth loading occurs at a point on part A'B' of the contact path.

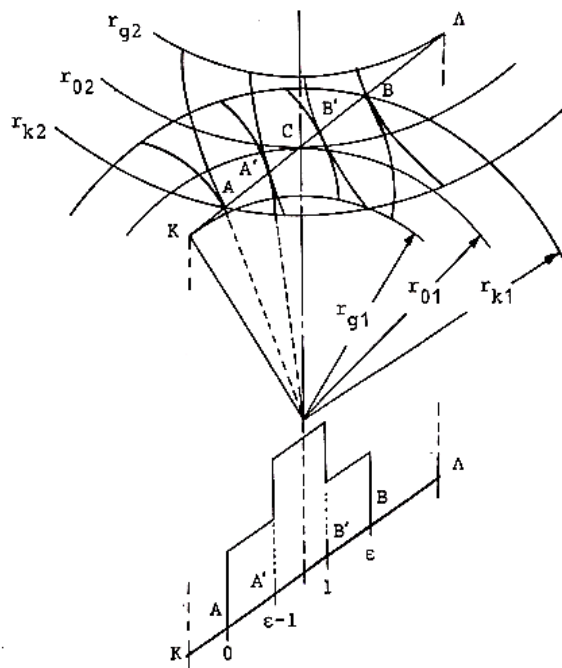


Fig. 4. (a) Gear teeth profiles of a gear transmission stage (b) Position of tooth load variation

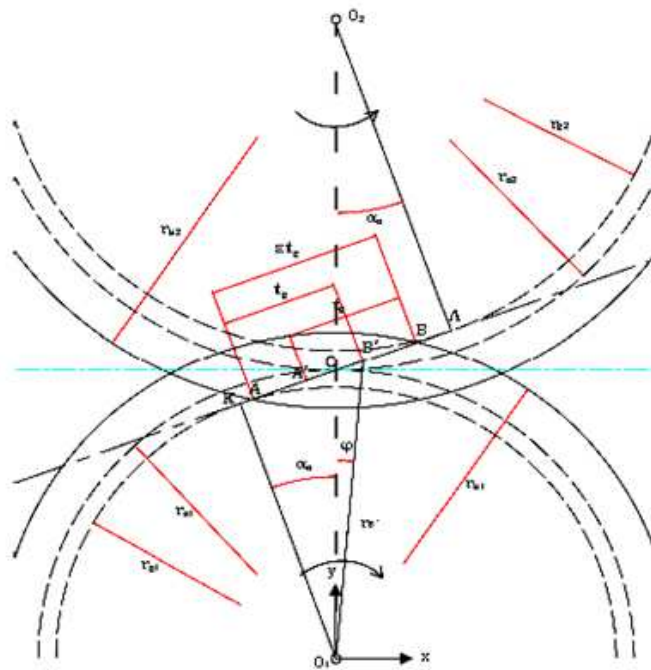


Fig. 5. Geometric determination of HPSTC

Table 1. Analytical data for each gear

Gear No	$z_1 = z_2$	m (mm)	P (KW)	n (rpm)	$M_t$ (Nm)
1	18	6	20	1250	131,78
2	20	10	20	1450	131,78
3	22	8	20	1250	131,78

Determination of the point of maximum stresses during gear meshing (Fig. 4), (Niemann, 1960; Spitas and Spitas, 2007; Costopoulos and Spitas, 2009), is as follows:

$$AB = \varepsilon \cdot t_g = AC + AB \quad (9)$$

$$AC = \sqrt{(r_{o2} + m)^2 - r_{o2}^2 \cdot \cos^2 \alpha_0} - r_{o2} \cdot \sin \alpha_0 \quad (10)$$

$$BC = \sqrt{(r_{o1} + m)^2 - r_{o1}^2 \cdot \cos^2 \alpha_0} - r_{o1} \cdot \sin \alpha_0 \quad (11)$$

Substituting Equation 10 and 11 to Equation 9 results Equation 12:

$$AB \sqrt{(r_{o2} + m)^2 - r_{o2}^2 \cdot \cos^2 \alpha_0} + \sqrt{(r_{o1} + m)^2 - r_{o1}^2 \cdot \cos^2 \alpha_0} - (r_{o1} + t_{o2}) \cdot \sin \alpha_0 \quad (12)$$

HPSTC is located at point B'. During parts AA' and BB' of the contact path, load is transmitted through two pairs of gear teeth, while during part A'B' only a single pair of gear teeth is subjected to the total load. The lengths of parts AB' and A'B equal the gear circular pitch,  $t_g$ , at the base circle. Thus, position of HSPTC is determined according to Fig. 5 as follows:

$$AC = \sqrt{(r_{o2} + m)^2 - r_{o2}^2 \cdot \cos^2 \alpha_0} - r_{o2} \cdot \sin \alpha_0 \quad (13)$$

$$CB' = AB' - AC = t_g - AC = \pi \cdot m \cdot \cos \alpha_0 - AC \quad (14)$$

Using triangle  $O_1B'C$ , (Spitas *et al.*, 2005; Spitas and Spitas, 2007; Raptis *et al.*, 2012), radius  $r_{B'}$  can be calculated according to the following Equation:

$$r_{B'} = \sqrt{r_{o1}^2 + CB'^2 - 2 \cdot r_{o1} \cdot CB' \cdot \cos(\alpha_0 + 90^\circ)} \quad (15)$$

Cartesians coordinates of point  $H$  are:  $(x, y) = (rB \sin\phi, rB \cos\phi)$

## Results and Discussion

### Bending Stress Finite Element Analysis

For the purposes of this investigation, computed Finite Element Analysis was used to simulate the loading of different gear teeth (Table 1), with one-tooth models fixed at their boundary (Fig. 6-8). For each tooth model, 11 loaded models have been analyzed.

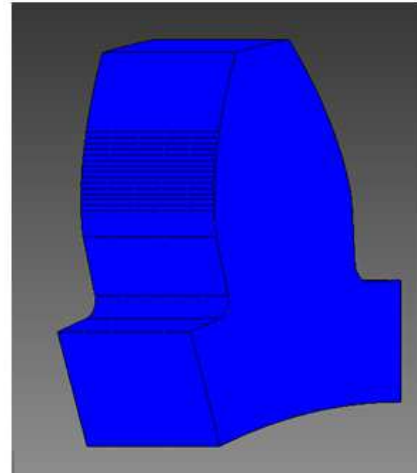


Fig. 6. Solid model structure

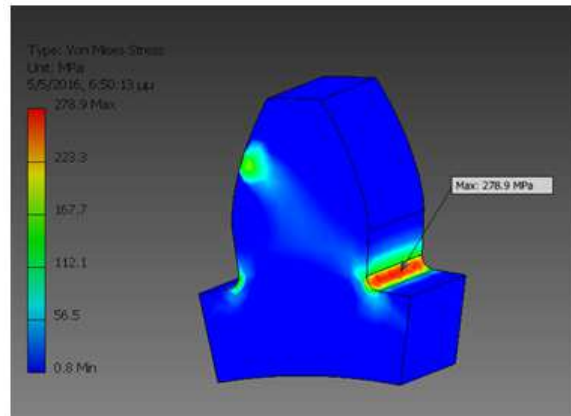


Fig. 7. Equivalent Stress at the HPSTC for  $m = 6$  mm model

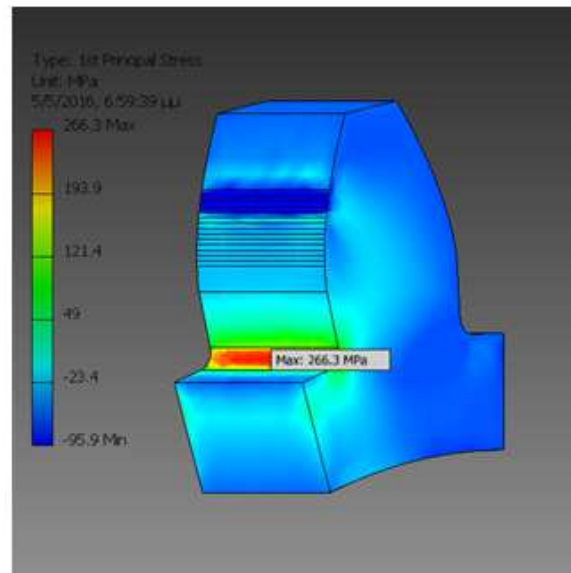


Fig. 8. 1st Principal Stress at the HPSTC for  $m = 6$  mm model



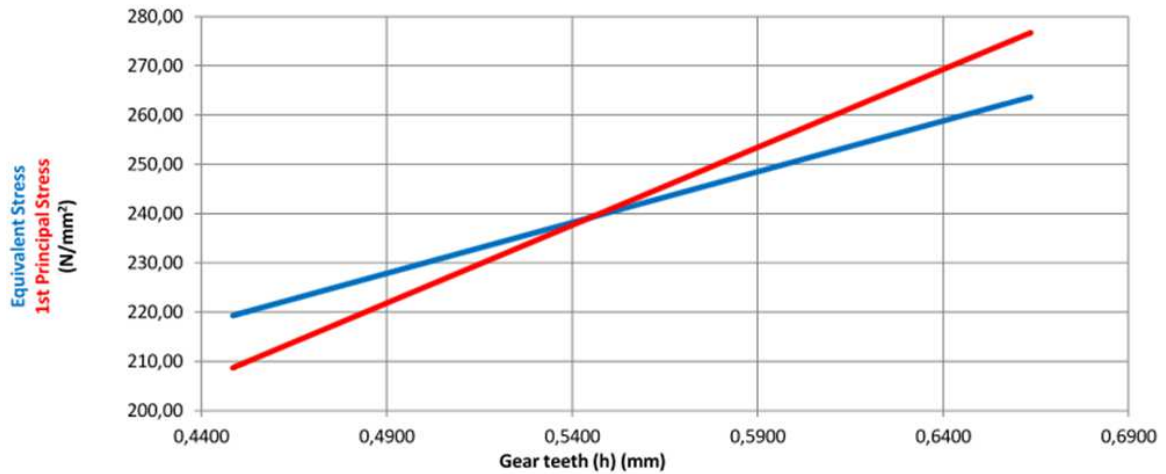


Fig. 9. Diagram between gear teeth h ratio and Equivalent - 1st Principal Stress ( $m = 6$  and  $z = 18$ ); Gear 2: ( $z_1 = z_2 = 20$ ,  $m = 10$ )

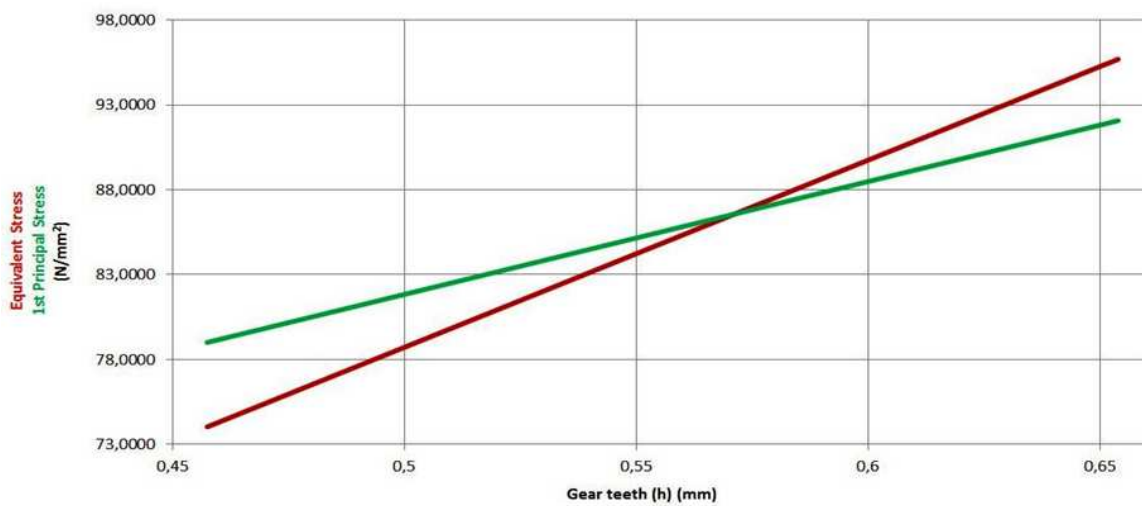


Fig. 10. Diagram between gear teeth h ratio and Equivalent - 1st Principal Stress ( $m = 8$  and  $z = 22$ )

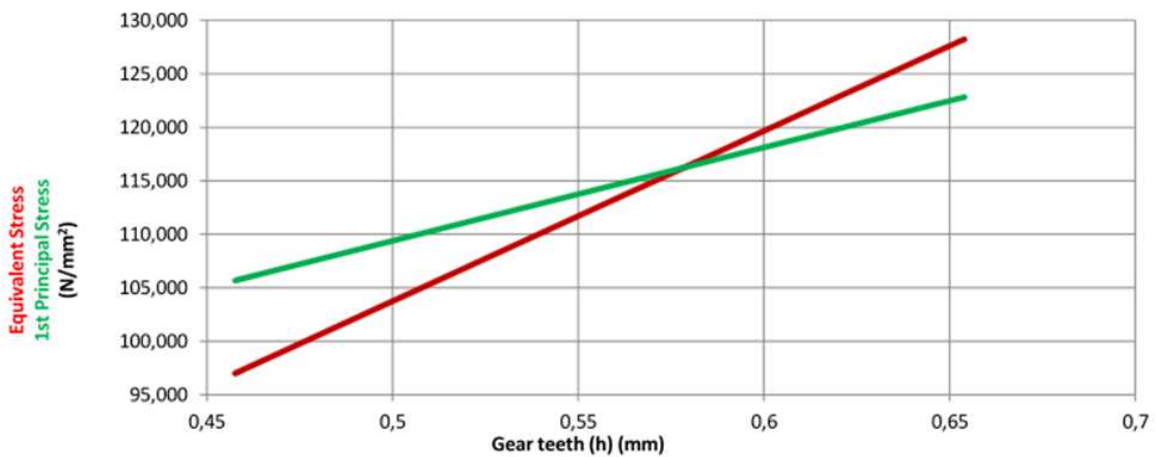


Fig. 11. Diagram between gear teeth h ratio and Equivalent - 1st Principal Stress ( $m = 10$  and  $z = 20$ )

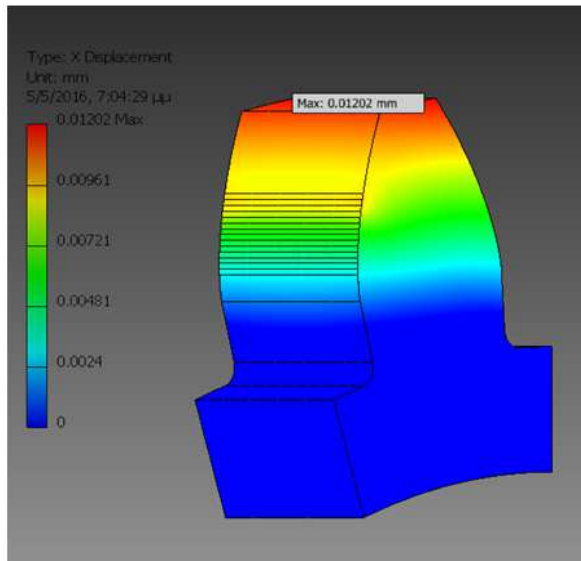


Fig. 12. x-Displacement at the HPSTC for m = 6 mm model

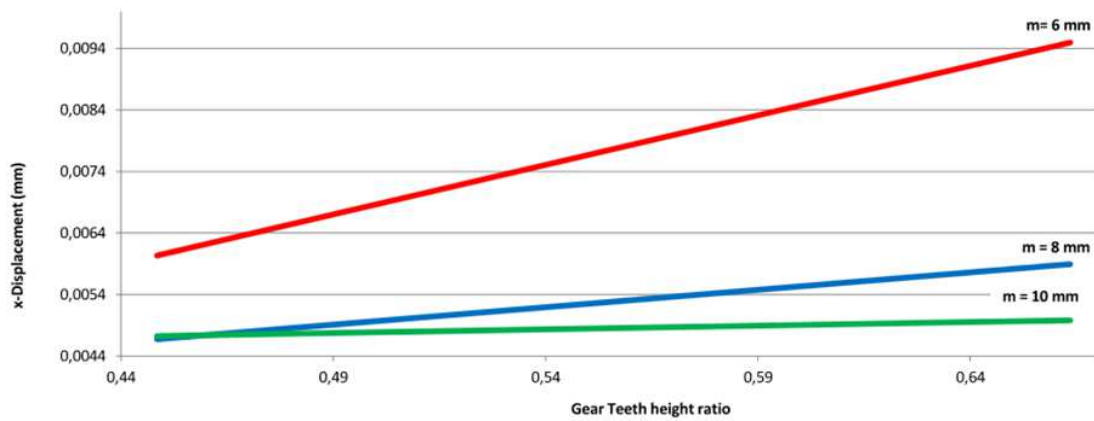


Fig. 13. Diagram between gear teeth height ratio and x displacement (mm)

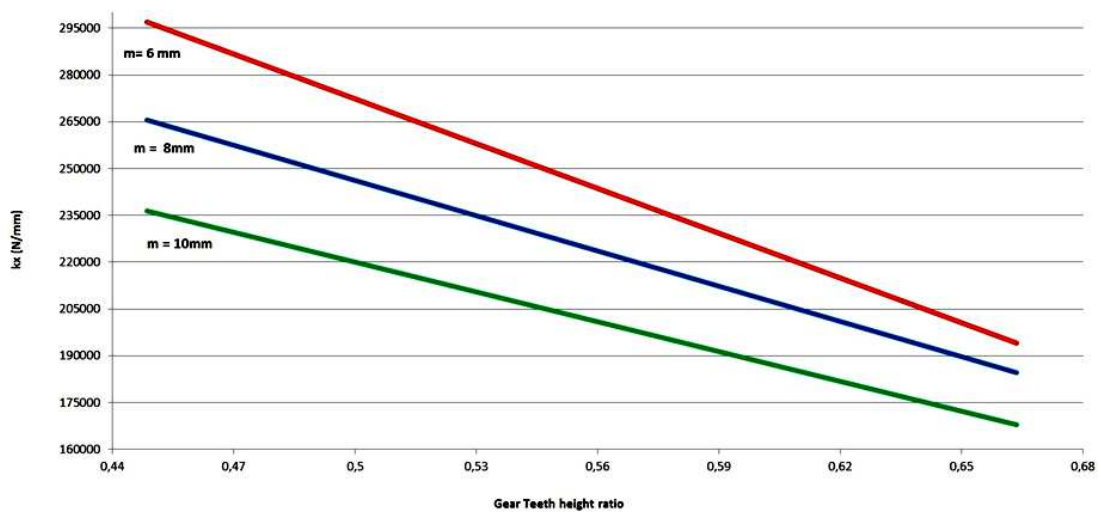


Fig. 14. Diagram between Gear Teeth Height ratio and Kx (N/mm)



Table 2. Parameters and FEA result values for m = 6 mm model

Contact distance from the gear 1 center (mm)	Pressure angle $\alpha^\circ$	Contact distance from the gear 2 center (mm)	Tangential Load Ft (N)	Equivalent Stress (N/mm <sup>2</sup> )	1 <sup>st</sup> Principal Stress (N/mm <sup>2</sup> )	Gear Teeth height ratio
52,72	15,739	55,56	2499,6	224,00	212,50	0.4485
53,00	16,794	55,28	2486,3	223,50	214,90	0.4700
53,29	17,778	54,99	2473,0	226,60	221,20	0.4915
53,57	18,702	54,71	2459,9	232,40	227,30	0.5130
53,86	19,575	54,42	2446,9	234,30	235,60	0.5345
54,14	20,403	54,14	2434,1	240,80	242,40	0.5561
54,42	21,192	53,86	2421,4	243,60	247,30	0.5776
54,71	21,947	53,57	2408,8	249,70	255,90	0.5991
54,99	22,670	53,29	2396,4	254,30	262,20	0.6206
55,28	23,364	53,00	2384,1	260,70	271,10	0.6421
55,56	24,033	52,72	2371,9	266,30	278,90	0.6636

Table 3. Parameters and FEA result values for m = 8 mm model

Contact distance from the gear 1 center (mm)	Pressure angle $\alpha^\circ$	Contact distance from the gear 2 center (mm)	Tangential Load Ft (N)	Equivalent Stress (N/mm <sup>2</sup> )	1st Principal Stress (N/mm <sup>2</sup> )	Gear Teeth height ratio
97,96	16,415	102,412	1345,228	75,57	79,60	0.4576
98,41	17,272	102,171	1339,145	76,12	80,32	0.4772
98,85	18,083	101,930	1333,117	77,70	81,15	0.4968
99,30	18,854	101,688	1327,142	79,92	82,68	0.5165
99,74	19,589	101,447	1321,221	82,32	83,90	0.5361
100,19	20,292	101,206	1315,353	84,53	85,22	0.5558
100,63	20,966	100,965	1309,536	86,27	87,13	0.5754
101,08	21,615	100,724	1303,771	89,88	88,71	0.5951
101,52	22,240	100,482	1298,056	91,56	89,29	0.6147
101,97	22,844	100,241	1292,391	93,82	90,69	0.6343
102,41	23,428	100,000	1286,775	95,95	92,14	0.6540

Table 4. Parameters and FEA result values for m = 10 mm model

Contact distance from the gear 1 center (mm)	Pressure angle $\alpha^\circ$	Contact distance from the gear 2 center (mm)	Tangential Load Ft (N)	Equivalent Stress (N/mm <sup>2</sup> )	1st Principal Stress (N/mm <sup>2</sup> )	Gear Teeth height ratio
86,45	16,960	89,91	1524,31	98,65	105,5	0.4528
86,80	17,693	89,56	1518,24	98,73	107,2	0.4730
87,14	18,392	89,22	1512,22	101,6	108,6	0.4933
87,49	19,061	88,87	1506,24	107,6	111,4	0.5135
87,84	19,704	88,53	1500,31	109,3	112,8	0.5337
88,18	20,322	88,18	1494,43	112,8	114,7	0.5540
88,53	20,917	87,84	1488,60	114,7	116,2	0.5742
88,87	21,493	87,49	1482,81	120,1	117,2	0.5944
89,22	22,050	87,14	1477,06	122,5	119,9	0.6146
89,56	22,590	86,80	1471,36	125,5	120,9	0.6349
89,91	23,113	86,45	1465,70	127,4	122,4	0.6551

Table 5. x Displacements versus tooth height ratio

m = 6 mm		m = 8 mm		m = 10 mm	
Gear Teeth height ratio	x Displacement at the point of contact (mm)	Gear Teeth height ratio	x Displacement at the point of contact (mm)	Gear Teeth height ratio	x Displacement at the point of contact (mm)
0.4485	0,0062	0.4576	0,0045	0.4528	0,0043
0.4700	0,0064	0.4772	0,0046	0.4730	0,0045
0.4915	0,0067	0.4968	0,0048	0.4933	0,0046
0.5130	0,0070	0.5165	0,0050	0.5135	0,0049
0.5345	0,0073	0.5361	0,0052	0.5337	0,0051
0.5561	0,0077	0.5558	0,0054	0.5540	0,0053
0.5776	0,0081	0.5754	0,0057	0.5742	0,0055
0.5991	0,0084	0.5951	0,0059	0.5944	0,0058
0.6206	0,0088	0.6147	0,0061	0.6146	0,0043
0.6421	0,0092	0.6343	0,0064	0.6349	0,0045
0.6636	0,0096	0.6540	0,0045	0.6551	0,0046

Table 6. Kx stiffness versus tooth height ratio

m = 6 mm		m = 8 mm		m = 10 mm	
Gear Teeth height ratio	Kx N/mm	Gear Teeth height ratio	Kx N/mm	Gear Teeth height ratio	Kx N/mm
0,4485	300077,3	0,4576	268695,7	0,4528	239620,3
0,47	288094	0,4772	260106,2	0,473	230847,3
0,4915	276312,9	0,4968	248801,7	0,4933	222297,3
0,513	264789,1	0,5165	239732,9	0,5135	214470,3
0,5345	253829,7	0,5361	231208,7	0,5337	207120,4
0,5561	243165,1	0,5558	222518,1	0,554	200450
0,5776	233273,7	0,5754	215052,9	0,5742	193890,5
0,5991	223867,2	0,5951	207588,6	0,5944	187619,9
0,6206	214536,4	0,6147	200769,4	0,6146	181698,8
0,6421	205877,3	0,6343	194290,1	0,6349	176027,1
0,6636	197327,2	0,654	188127,5	0,6551	170298,5

### Bending Deflection Finite Element Analysis

For bending deflection calculation the x Displacement at the point of contact values computed for all the single tooth models. Since the loading forces distributed to a mirror four lanes facial area which, as described, the effect of Hertz deflection was diminished, the value of the x Displacement derived from FEA at the contact point representing the circumference bending deflection with good approximation.

### Stiffness Estimation

Finite element contact between pinion and wheel tooth pairs is not taken into account (Chaari *et al.*, 2009). In order to find the singular stiffness of one tooth of the pinion, we follow the same load analysis as we have already described in chapter Materials and Methods.

In order to find the singular stiffness of one tooth of the pinion, a linear distributed force  $F$ , which simulates the action of the meshing tooth of the wheel, is applied to the tooth flank normal to the involute profile and along the line of action at the appropriate nodes. This force is introduced by its two projections on  $x$  axis and  $y$  axis. Two deflections  $\delta x$  and  $\delta y$  are obtained and the deflection of the tooth along the direction of the force is given by:

$$\delta = \delta x \cos(\alpha_m) + \delta y \sin(\alpha_m) \quad (16)$$

where,  $\alpha_m$  is the operating pressure angle.

The single stiffness of the tooth is then obtained by:

$$K_x = Fu / \delta x \quad (17)$$

Taking into account the data of Table 2-4, we identify single stiffness  $K_x$  of the tooth, due ratio (17).

### Conclusion

In this study a discrete loading model of gears' teeth was created and analyzed with method with application of FEA software. The mesh load was applied in discrete

loading lanes all along the tooth contact surface from the LPSTC to the HPSTC.

From the simulation of three different modul teeth, it eventuates (Table 5 and 6, Fig. 14).

- The root bending stresses
- The bending displacements at the points of contact

Subsequently, evaluating the bending displacements data, the peripheral stiffness of each modeled tooth was calculated.

The outcome results are presented in graphs versus the ratio of the contact point height to the total tooth height. The main conclusion that firstly all the above magnitudes shows linear distribution as the contact point moves from LPSTC to the HPSTC and secondly the bending stress and the deflection are in linearly proportional to gear teeth height ratio.

### Author's Contributions

**Antonios D. Tsolakis:** Participated in all experiments coordinated the data-analysis.

**Konstantinos G. Raptis:** Contributed to the writing of the manuscript.

**Maria D. Margaritou:** Designed the research plan and organized the study.

### Ethics

This article is original and contains unpublished material. The corresponding author confirms that all of the other authors have read and approved the manuscript and no ethical issues involved.

### References

- Chaari, F., T. Fakhfakh and M. Haddar, 2009. Analytical modelling of spur gear tooth crack and influence on gearmesh stiffness. *Eur. J. Mechan. A/Solids*, 28: 461-468.  
 DOI: 10.1016/j.euromechsol.2008.07.007

- Costopoulos, T. and V. Spitas, 2009. Reduction of gear fillet stresses by using one-sided involute asymmetric teeth. *J. Mechan. Mach. Theor.*, 44: 1524-1534.  
DOI: 10.1016/j.mechmachtheory.2008.12.002
- DIN 3990, 1987. Calculation of load capacity of cylindrical gears. Deutsches Institut für Normung E.V.
- Dolan, T.J. and E.L. Broghamer, 1942. A photo-elastic study of stress in Gear tooth fillets. *Univ. Ill. Eng. Exp. Sta. Bull.*
- Fakher, C., F. Tahar and H. Mochamed, 2009. Analytical modelling of spur gear tooth crack and influence on gearmesh stiffness. *Eur. J. Mechan.*, 28: 461-468.  
DOI: 10.1016/j.euromechsol.2008.07.007
- Heywood, R.B., 1962. Designing against Fatigue of Metals. 1st Edn., Reinhold Publishing Corporation, pp: 436.
- ISO 6336:3, 1996. Calculation of the load capacity of spur and helical gears Part 3: Calculation of tooth bending strength.
- Kawalec, A., J. Wiktor and D. Ceglarek, 2006. Comparative analysis of tooth-root strength using ISO and AGMA standards in spur and helical gears with FEM-based verification. *J. Mech. Des.*, 128: 1141-1158. DOI: 10.1115/1.2214735
- Lewis, W., 1882. Investigation of strength of gear teeth. *Proceedings of the Engineering Club No. 1, (EC' 82), Philadelphia.*
- Niemann, G., 1982. Machine Elements: Gears. 1st Edn., Springer-Verlag, Berlin, ISBN-10: 3540033785.
- Niemann, G., 1960. *Maschinelemente II, Band 2.* 1st Edn., Springer-Verlag, ISBN-10: 3-540-03378-5, pp: 97.
- Raptis, K., T. Costopoulos and A. Tsolakis, 2012. Comparison between Niemann's and finite element method for the estimation of maximum allowable stress of meshing spur gear teeth at highest point of single tooth contact. *Am. J. Eng. Applied Sci.*, 5: 205-216. DOI: 10.3844/ajeassp.2012.205.216
- Raptis, K., T. Costopoulos, G. Papadopoulos and A. Tsolakis, 2010. Rating of spur gear strength using photoelasticity and the finite element method. *Am. J. Eng. Applied Sci.*, 3: 222-231.  
DOI: 10.3844/ajeassp.2010.222.231
- Spitas, V. and C. Spitas, 2007. Numerical and experimental comparative study of strength-optimised AGMA and FZG spur gears. *Acta Mech.*, 193: 113-126. DOI: 10.1007/s00707-006-0384-x
- Spitas, V., T. Costopoulos and C. Spitas, 2005. Increasing the strength of standard involute gear teeth with novel circular root fillet design. *Am. J. Applied Sci.*, 2: 1058-1064.  
DOI: 10.3844/ajassp.2005.1058.1064
- Tsolakis, A. and K. Raptis, 2011. Comparison of maximum gear-tooth operating bending stresses derived from Niemann's analytical procedure and the finite element method. *Am. J. Eng. Applied Sci.*, 4: 342-346. DOI: 10.3844/ajeassp.2011.350.354